



The use of mechanistic descriptions of algal growth and zooplankton grazing in an estuarine eutrophication model

M.E. Baird^{a,*}, S.J. Walker^{a,b}, B.B. Wallace^a, I.T. Webster^a, J.S. Parslow^b

^aCSIRO Land and Water, P.O. Box 1666, Canberra, Australian Capital Territory 2601, Australia

^bCSIRO Marine Research, P.O. Box 1538, Hobart, Tasmania 7001, Australia

Received 22 October 2001; received in revised form 15 April 2002; accepted 15 April 2002

Abstract

A simple model of estuarine eutrophication is built on biomechanical (or mechanistic) descriptions of a number of the key ecological processes in estuaries. Mechanistically described processes include the nutrient uptake and light capture of planktonic and benthic autotrophs, and the encounter rates of planktonic predators and prey. Other more complex processes, such as sediment biogeochemistry, detrital processes and phosphate dynamics, are modelled using empirical descriptions from the Port Phillip Bay Environmental Study (PPBES) ecological model. A comparison is made between the mechanistically determined rates of ecological processes and the analogous empirically determined rates in the PPBES ecological model. The rates generally agree, with a few significant exceptions. Model simulations were run at a range of estuarine depths and nutrient loads, with outputs presented as the annually averaged biomass of autotrophs. The simulations followed a simple conceptual model of eutrophication, suggesting a simple biomechanical understanding of estuarine processes can provide a predictive tool for ecological processes in a wide range of estuarine ecosystems.

© 2003 Elsevier Science B.V. All rights reserved.

Keywords: eutrophication; numerical model; macroalgae; seagrass; phytoplankton; zooplankton; size; diffusion layers

1. Introduction

Eutrophication is the process of accelerated production of organic matter, particularly algae, in a water body, usually as a result of increasing nutrient inputs (Bricker, Clement, Pirhalla, Orlando, & Farrow, 1999; Nixon, 1995). Eutrophication is an increasing problem in rivers, lakes and estuaries throughout the world, resulting in the deterioration of the aquatic environment (Chorus & Bartram, 1999). In the estuarine environment the most commonly observed effect of eutrophication is a general shift from large, slow-growing marine plants (seagrass and benthic macroalgae) towards fast-growing algae (Harris et al., 1996). A more detailed analysis of

the effects of eutrophication can be found in Cloern (2001).

The last decade or so has seen the publication of a large number of process-based numerical models of estuarine ecology (for example Hamilton & Schladow, 1997; Madden & Kemp 1996; Murray & Parslow, 1997). These deterministic models are based on mathematical descriptions of the processes (such as phytoplankton growth, zooplankton grazing, etc.) which are considered most important in determining ecological behaviour. In large multi-disciplinary studies of estuaries (such as Chesapeake Bay, USA or Port Phillip Bay, Australia), extensive field experiments and measurements allow ecologically important processes to be accurately modelled using empirical relationships (such as the Monod growth equation). When the empirical processes are combined to form a dynamic model, only a small subset of parameters are unknown (typically those relating to higher trophic level loss terms). The unknown parameters are then calibrated to field data (Steele &

* Corresponding author. School of Mathematics, UNSW, Sydney, New South Wales 2052, Australia.

E-mail address: mbaird@maths.unsw.edu.au (M.E. Baird).

Clark, 1998). This approach has led to important discoveries about ecosystem function (i.e. denitrification in Port Phillip Bay), and aided in management decisions (Harris et al., 1996).

Only a few of the Australian continent's approximately 1000 estuaries have extensive field programmes capable of obtaining accurate empirical approximations of the critical ecological processes. The use of empirical approximation in the data-poor estuaries requires extrapolation from estuaries with possibly different physical environments and biota. Alternatively, it is possible to replace some empirical descriptions of ecological processes with more mechanistic descriptions (Baird & Emsley, 1999). At the scale of ecological processes, mechanistic is used to refer to the method of equation development. For example, using the process of diffusion to the cell surface to describe nutrient uptake is considered mechanistic because it uses a well-understood physical law (Fick's law of diffusion), and contains physically meaningful parameters such as the diffusion coefficient and the geometry of the cell (Pasciak & Gavis, 1975). The use of mechanistic descriptions of ecological processes reduces the need for extrapolation of model parameters to simulate ecological processes in data-poor estuaries.

This paper develops a model of estuarine eutrophication that is built on mechanistic descriptions of a number of the key ecological processes in estuaries. To assess the model's performance, two comparisons are made. First, the mechanistically determined rates of ecological processes are compared to the analogous processes in the Port Phillip Bay Environmental Study (PPBES) ecological model. This first comparison sheds light on both the mechanistic model's ability to capture dynamical behaviour of the system, and the PPBES model's empirical representation of ecological processes. Secondly, the mechanistic model's performance is compared to a conceptual model of estuarine eutrophication over a range of estuarine depths and nutrient loads.

2. Model derivation

The model developed here is a modification of the ecological model used in the PPBES (Murray & Parslow, 1997). A number of compartments of the model are unchanged (such as sediment nitrogen cycling), while other sections (in particular, autotroph growth) have fundamentally changed. To remain concise, this paper will detail only the components of the model that have fundamentally changed: the equations for light attenuation through the water, autotroph growth (both benthic and planktonic) and zooplankton grazing. A more complete description of the model listing equations and parameter values is available (<http://www.marine.csiro.au/serm/ecology.pdf>).

2.1. Light attenuation

In the model, light is attenuated through the water column, the benthic macroalgae, the seagrass and the microphytobenthos sequentially. Photosynthetically available radiation (PAR) at the bottom of a layer of water, I_{bot} (mol photon $\text{m}^{-2} \text{s}^{-1}$), is approximated by:

$$I_{\text{bot}} = I_{\text{top}} e^{-K_d dz} \quad (1)$$

where I_{top} is the PAR at the top of the layer (mol photon $\text{m}^{-2} \text{s}^{-1}$), dz the thickness of the layer (m) and K_d is the total attenuation coefficient of the water (m^{-1}). K_d is given by the sum of the each attenuating component in the water:

$$K_d = k_w + n_{\text{PS}} \overline{aA}_{\text{PS}} + n_{\text{PL}} \overline{aA}_{\text{PL}} + n_{\text{MPB}} \overline{aA}_{\text{MPB}} + k_{\text{other}} \quad (2)$$

where k_w is the background attenuation coefficient of water (m^{-1}), n_{PS} , $\overline{aA}_{\text{PS}}$, n_{PL} , $\overline{aA}_{\text{PL}}$ and n_{MPB} and $\overline{aA}_{\text{MPB}}$ are the water column concentration (cell m^{-3}) and absorption cross-section ($\text{m}^2 \text{cell}^{-1}$) of cells of small phytoplankton, large phytoplankton and microphytobenthos, respectively, and k_{other} is the attenuation coefficient due to other components in the water column (such as dissolved organic nitrogen or suspended solids) (m^{-1}). While not modelled explicitly here, it is worth noting in sediment laden estuaries, k_{other} can be the dominant attenuating component of the water column. The average irradiance in the layer, I_{av} (mol photon $\text{m}^{-2} \text{s}^{-1}$), is given by:

$$I_{\text{av}} = \frac{I_{\text{top}} - I_{\text{bot}}}{K_d dz} \quad (3)$$

In the model, light reaching the benthos is first attenuated by macroalgae, and then seagrass. The light below the macroalgae and seagrass, respectively, is given by:

$$I_{\text{below MA}} = I_{\text{bot}} e^{-MA \overline{aA}_{\text{MA}}} \quad (4)$$

$$I_{\text{below SG}} = I_{\text{below MA}} e^{-SG \overline{aA}_{\text{SG}}} \quad (5)$$

where MA and SG are the biomass (mg N m^{-2}); and $\overline{aA}_{\text{MA}}$ and $\overline{aA}_{\text{SG}}$ are the biomass-specific absorption cross-sections ($\text{mg N}^{-1} \text{m}^2$) of the macroalgae and seagrass, respectively. The PPBES ecological model considered the reduced growth rate of seagrass due to epiphytes. In this paper, epiphytes are considered to be part of the benthic macroalgae. Epiphytes and macroalgae both receive light before seagrass, and sharing the same surface, have a similar effective benthic boundary layer thickness. As epiphytes and macroalgae have similar maximum supply rates of nutrient and light, and shade seagrass in a similar manner, the use of one class of autotroph for both seemed reasonable.

Finally, the remaining light passes through a thin layer of microphytobenthos at the surface of the sediment:

$$I_{\text{below MPB}} = I_{\text{below SG}} e^{-n_{\text{MPB}} \overline{a}_{\text{MPB}} dz} \quad (6)$$

where n_{MPB} is the concentration of microphytobenthos cells (cell m^{-3}) with an absorption cross-section of $\overline{a}_{\text{MPB}}$ ($\text{m}^2 \text{cell}^{-1}$) in a sediment layer dz thick (m). By including only attenuation due to microphytobenthos in Eq. (6) it is assumed that the microphytobenthos lie in the surface layer of the sediment. The average light flux available to the microphytobenthos cells is given by:

$$I_{\text{av}} = \frac{I_{\text{below SG}} - I_{\text{below MPB}}}{n_{\text{MPB}} \overline{a}_{\text{MPB}} dz} \quad (7)$$

The above description of the light field in an estuarine environment is significantly different from that employed in the PPBES ecological model, and other aquatic ecological models (Fasham, Ducklow, & McKelvie, 1990; Madden & Kemp, 1996). Autotroph absorption cross-sections have been used to parameterize both the dependence of autotroph growth rate on light availability (see Eqs. (9) and (12)), and the attenuation of light as it passes through the water column and benthos (Eqs. (2) and (4–6)).

2.2. Autotroph growth

The growth rate of each autotroph is determined from a functional form specifying the interaction of the maximum supply rates of nutrients and light, and the maximum growth rate (called the CR model in Baird, Emsley, & McGlade, 2001). Maximum supply rates of nutrients and light are based on physical limits which will be derived below. Maximum supply rates determine the initial slope of the nutrient or light versus growth curve. Note that this is fundamentally different from the typical Monod or Michaelis–Menton type growth functions, which use empirically determined half-saturation constants to determine the shape of the curve. This CR model approach is preferred because maximum supply rates of nutrients and light can be calculated mechanistically from physical laws, without the need for extensive calibration of parameter values. The CR model requires the determination of the maximum growth rate, μ^{max} , and the maximum supply rates of nutrients, k_N , and light, k_I , and the elemental ratios (or stoichiometry) of each autotroph.

2.2.1. Maximum uptake rates of algal cells suspended in the water column

Algal cells suspended in the water column (phytoplankton) obtain nutrients from the surrounding fluid, and light as a function of the average light in the layer

in which they are suspended. A physical limit to the rate at which a cell can absorb nutrients is given by the rate at which nutrient molecules can diffuse from the surrounding fluid to the cell surface, called the mass transfer limit (Pasciak & Gavis, 1975), and has been used in this paper as the maximum rate of nutrient uptake. For a perfectly absorbing cell, the mass transfer limit, k_N ($\text{mol cell}^{-1} \text{s}^{-1}$), is given by:

$$k_N = \psi DN \quad (8)$$

where ψ is the diffusion shape factor (m cell^{-1}), D the molecular diffusivity of the nutrient ($\text{m}^2 \text{s}^{-1}$) and N is the concentration of the nutrient in the water column (mol m^{-3}). ψ for a sphere is $4\pi r$, where r is the cell radius (m).

The maximum supply rate of light, k_I ($\text{mol photon cell}^{-1} \text{s}^{-1}$), is given by:

$$k_I = I_{\text{av}} \overline{a}_{\text{cell}} \quad (9)$$

where $\overline{a}_{\text{cell}}$ is the absorption cross-section of a cell ($\text{m}^2 \text{cell}^{-1}$), and I_{av} is the average PAR in the layer (Eq. (3)) ($\text{mol photon m}^{-2} \text{s}^{-1}$). The absorption cross-section of a spherical cell is given by Kirk (1975):

$$\overline{a}_{\text{cell}} = \pi r^2 \left(1 - \frac{2(1 - (1 + 2\overline{\gamma C}r) e^{-2\overline{\gamma C}r})}{(2\overline{\gamma C}r)^2} \right) \quad (10)$$

where $\overline{\gamma C}$ is the absorption coefficient (m^{-1}). $\overline{\gamma C}$ is the rate (per metre travelled through the cell) at which light is attenuated. The diffusion shape factor and absorption cross-section of more complicated shapes can be found in Baird & Emsley (1999).

2.2.2. Maximum uptake rates of benthic macroalgae

Benthic macroalgae reside on the top of the sediment, take nutrients out of the water column, and are exposed to light that reaches the bottom of the water column. Like nutrient uptake to algal cells, the supply rate of nutrients to benthic surfaces also has a mass transfer limit (Sanford & Crawford, 2000). Both the mass transfer limit, and the biomass of macroalgae, are quantified per square metre. The maximum rate of nutrient uptake to benthic macroalgae, k_N ($\text{mol m}^{-2} \text{s}^{-1}$), can be calculated as a diffusion rate through an effective diffusive boundary layer thickness, δ (m):

$$k_N = \frac{D}{\delta} N \quad (11)$$

where D is the molecular diffusivity of the nutrient ($\text{m}^2 \text{s}^{-1}$), and N is the concentration of the nutrient in the water column (mol m^{-3}). The effective thickness of the diffusive boundary layer, δ , is strongly influenced by shear stress (itself a function of surface roughness and water velocity) at the water–benthos interface (Hurd, 2000). For typical hydrodynamic environments of aquatic benthos, the effective diffusive boundary

layer thickness is of the order of 0.1 mm for a typical benthic macrophyte (0.22–0.68 mm for oxygen transfer in lake periphyton [(Riber & Wetzel, 1987) and 0.04–0.15 mm for CO₂ transport in seagrass (Smith & Walker, 1980)].

The maximum light capture by the macroalgae, k_I (mol photon m⁻² s⁻¹), is given by:

$$k_I = I_{\text{bot}}(1 - e^{-\overline{aA}_{\text{MA}}\text{MA}}) \quad (12)$$

where I_{bot} is the incident radiation at the top of the macroalgae (Eq. (1)) (mol photon m⁻² s⁻¹), MA the biomass of macroalgae (mg N m⁻²) and $\overline{aA}_{\text{MA}}$ is the nitrogen-specific absorption cross-section of macroalgae (m² mg N⁻¹). This approach is similar to that used by modellers of terrestrial canopies: it is assumed that the projected area of the benthos is fully covered by the macroalgae, but the macroalgae has varying thickness, and therefore, absorbance depending on the biomass.

2.2.3. Maximum uptake rates of seagrass

In the model, seagrass obtain nutrients from the sediment, and light after it has passed through the water column and benthic macroalgae. The present understanding of nutrient uptake through a root system was considered too limited to justify a mechanistic determination of the maximum uptake rate. Instead, a maximum supply rate was ‘back-calculated’ from a half-saturation constant and a maximum growth rate obtained from the PPBES ecological model using:

$$k_N = \frac{\text{SG}\mu^{\text{max}}}{K_{1/2}}N \quad (13)$$

where SG is the biomass of seagrass (mol N m⁻²), μ^{max} the maximum growth rate (s⁻¹), N the sediment porewater nutrient concentration (mol m⁻³), and $K_{1/2}$ is an experimentally determined half-saturation constant of nutrient-limited growth when fitted to the Monod growth equation (mol N m⁻³). The implication of the last equation is that the rate of nutrient uptake per square metre increases with biomass. The increase in uptake with biomass is probably realistic, as a higher biomass of seagrass would have a larger root system (in the same way that a higher biomass of phytoplankton cells would have a larger surface area). The maximum rate of light uptake by seagrass is obtained by the same method as macroalgae (Eq. (12)).

2.2.4. Maximum uptake rates of benthic microalgae

Benthic microalgae are suspended in the top layer of the sediment. The maximum nutrient uptake (from the sediment porewater) takes the same form as for suspended algal cells, $k_N = \psi DN$, although the diffusion

coefficient is reduced by the longer diffusional pathways required for diffusion in a porous medium:

$$D_{\text{porewater}} = \frac{\vartheta D}{\theta} \quad (14)$$

where ϑ is the porosity, and θ is the tortuosity (both dimensionless), which can be approximated by $\theta = 1 - \ln(\vartheta^2)$ (Boudreau, 1996). Light capture by microphytobenthos is modelled using Eqs. (7) and (9) as for algal cells suspended in the water column.

2.2.5. Growth rates of autotrophs based on maximum uptake rates and a maximum growth rate

It is not possible to continue a mechanistic approach to modelling intracellular autotrophic processes, which are well studied, but far more complex than the extracellular processes described above. Instead, to combine the effects of extracellular physical limits to nutrient and light uptake with a maximum growth rate, an empirical approach is undertaken (the comparison with data is found in Baird et al., 2001). This empirical approach is somewhat different from other growth models (such as Droop, 1968). We justify the introduction of a new growth model scheme because it allows the logical use of mechanistically determined maximum uptake rates and the maximum growth rate to determine an autotroph’s growth rate. The derivation takes two slightly different paths, depending on whether biomass is quantified per cubic metre, as for planktonic (suspended) autotrophs, or per square metre, as for benthic plants.

2.2.6. Planktonic autotrophs

For planktonic autotrophs, the uptake rate of nutrients and light is assumed to be a linear function of the resource already stored (although light cannot be stored, energy from light can be stored as fixed carbon). For a light- and a single nutrient-limited system, uptake of

$$N = k_N \left(\frac{R_N^{\text{max}} - R_N}{R_N^{\text{max}}} \right) \text{mol N cell}^{-1} \text{s}^{-1} \quad (15)$$

and

$$I = k_I \left(\frac{R_I^{\text{max}} - R_I}{R_I^{\text{max}}} \right) \text{mol photon cell}^{-1} \text{s}^{-1} \quad (16)$$

where R (mol cell⁻¹) are reserves of a nutrient and light available for growth, and R^{max} represents the maximum values of R . Now assume that growth rate, μ^{max} (s⁻¹), is determined by the product of the reserves of both light and the nutrient:

$$\mu = \mu^{\text{max}} \frac{R_N}{R_N^{\text{max}}} \frac{R_I}{R_I^{\text{max}}} \quad (17)$$

where μ^{max} is the maximum growth rate of a cell (s⁻¹). The quantity of a nutrient or energy in a cell is given by $\mu(m + R)$, where m is the stoichiometry coefficient

specifying the number of moles per cell when the reserves are zero. In other studies m is sometimes referred to as the minimum quota. m is obtained from a cell radius, r (m) and the cell radius to cellular carbon content relationship of Strathmann (1967) given in Hofmann et al. (2000), multiply by the Redfield ratio of that nutrient to carbon ($= m_N/m_C$):

$$m_N = 1.32((4/3)\pi r^3)^{0.758} (m_N/m_C) \text{ mol N cell}^{-1} \quad (18)$$

The quantity of a nutrient or photons required to maintain a growth rate of μ (s^{-1}) is $\mu(m + R)$ ($\text{mol cell}^{-1} \text{s}^{-1}$). To determine the growth rate at a particular combination of k_I , k_N and μ^{max} , a steady-state solution is obtained by equating uptake and consumption of each nutrient (or light):

$$k_N \left(\frac{R_N^{\text{max}} - R_N}{R_N^{\text{max}}} \right) = \mu^{\text{max}} (m_N + R_N) \frac{R_N}{R_N^{\text{max}}} \frac{R_I}{R_I^{\text{max}}} \quad (19)$$

$$k_I \left(\frac{R_I^{\text{max}} - R_I}{R_I^{\text{max}}} \right) = \mu^{\text{max}} (m_I + R_I) \frac{R_N}{R_N^{\text{max}}} \frac{R_I}{R_I^{\text{max}}} \quad (20)$$

where m_N and m_I are stoichiometry coefficients specifying the number of moles of N and photons per cell. For simplicity, we have set the maximum capacity of the nutrient reserves to equal that of the minimum quota ($R^{\text{max}} = m$). While this may be appropriate for carbon, other nutrients can be stored by cells in quantities much greater than the minimum quota (i.e. Vitamin B12 Droop, 1968). Approximating R^{max} by m is not limiting in this paper because we consider only steady-state growth of cells (so there is no explicit intracellular storage of nutrients). For planktonic autotrophs the units of m , R , R^{max} and k are per cell.

2.2.7. Benthic autotrophs

For benthic autotrophs, uptake of nutrients and light are also assumed to be a linear function of stored reserves, although the units of uptake have changed. Uptake of

$$N = k_N \left(\frac{R_N^{\text{max}} - R_N}{R_N^{\text{max}}} \right) \text{ mol N m}^{-2} \text{ s}^{-1} \quad (21)$$

$$k_I \left(\frac{R_I^{\text{max}} - R_I}{R_I^{\text{max}}} \right) \text{ mol photon m}^{-2} \text{ s}^{-1} \quad (22)$$

For benthic autotrophs, the balance between growth and uptake becomes:

$$k_N \left(\frac{R_N^{\text{max}} - R_N}{R_N^{\text{max}}} \right) = \mu^{\text{max}} m_N \frac{R_N}{R_N^{\text{max}}} \frac{R_I}{R_I^{\text{max}}} \quad (23)$$

$$k_I \left(\frac{R_I^{\text{max}} - R_I}{R_I^{\text{max}}} \right) = \mu^{\text{max}} m_I \frac{R_N}{R_N^{\text{max}}} \frac{R_I}{R_I^{\text{max}}} \quad (24)$$

The units of m , R , R^{max} and k are all per square metre for benthic autotrophs. m and R^{max} are equal to the

biomass of the benthic autotroph. The CR model for benthic autotrophs has not yet been compared to empirical data, although studies like Fong, Kamer, Boyer, and Boyle (2001) introduce this possibility, and allude to the influences of the diffusive boundary layer. The difference between benthic and planktonic formulations arises because planktonic reserves are specified per cell, with the number of cells changing, while benthic reserves are specified per unit area, with area being constant. As a result, to balance nutrient uptake with growth, uptake equals μm for benthic autotrophs, but $\mu(m + R)$ for planktonic autotrophs.

To obtain a growth rate, μ , from Eq. (17) requires knowledge of R_N and R_I (and parameters R_N^{max} and R_I^{max}). Ideally, in an ecological model R_N and R_I will be state variables, with their values tracked through time (as in Baird & Emsley, 1999). However, with five autotrophs this is computationally expensive. Instead, if it is assumed that the autotroph has reached an equilibrium growth state (which we have already done by equating uptake with growth in Eqs. (19), (20), (23) and (24)), R_N and R_I can be determined at every time point if μ^{max} , m_I , m_N , k_N and k_I are known. The equilibrium state is obtained by solving two non-linear simultaneous equations (Eqs. (19) and (20) for planktonic autotrophs and Eqs. (23) and (24) for benthic autotrophs) (Baird & Emsley, 1999, p. 111). Again, this is a computationally expensive procedure. However, if the rates are non-dimensionalized, a generic look-up table can be created, and the solution of the simultaneous equations quickly referenced.

2.3. Planktonic grazing

In the model, large zooplankton graze on large phytoplankton and microphytobenthos, while small zooplankton graze on small phytoplankton. Grazing rates are determined as the minimum of the maximum growth rate of the zooplankton (i.e. how quickly the prey can be ingested) and the maximum encounter rate between the predator and prey. Maximum growth rate of small and large zooplankton are parameters (Table 1). The maximum encounter rates between predators and prey are calculated based on summing the rectilinear encounter rate of spheres due to three processes: diffusion, relative motion (swimming and sinking) and fluid shear (Baird & Emsley, 1999, Table 2). The encounter rate between one predator and a population of prey cells ($\text{cell (P)} \text{s}^{-1}$) is given by:

$$\text{encounter rate} = n_P \varphi_{Z,P} \quad (25)$$

where $\varphi_{Z,P}$ is the encounter rate coefficient between species Z and P ($\text{m}^3 \text{s}^{-1}$) (Baird & Emsley, 1999), and n_P is the concentration of prey cells ($\text{cell (P)} \text{m}^{-3}$).

Table 1
List of parameter values used in the mechanistic formulations

Parameter	Symbol	Units	Value
Background light attenuation coefficient	k_w	m^{-1}	0.3
DON-specific light attenuation coefficient	k_{DON}	$m^{-1} (mg N m^{-3})^{-1}$	$9 e-4$
Detrital N specific light attenuation coefficient	k_{DL}	$m^{-1} (mg N m^{-3})^{-1}$	$3.8 e-3$
TSS specific light attenuation coefficient	k_{TSS}	$m^{-1} (kg m^{-3})^{-1}$	30.0
Absorption cross-section of macroalgae	\overline{aA}_{MA}	$m^2 mg N^{-1}$	$1 e-3$
Absorption cross-section of seagrass	\overline{aA}_{SG}	$m^2 mg N^{-1}$	$1 e-5$
Absorption coefficient of large phytoplankton	$\overline{\gamma C}_{LP}$	m^{-1}	50,000
Absorption coefficient of small phytoplankton	$\overline{\gamma C}_{SP}$	m^{-1}	50,000
Absorption coefficient of microphytobenthos	$\overline{\gamma C}_{MPB}$	m^{-1}	50,000
Maximum growth rate of macroalgae	μ_{MA}^{max}	d^{-1}	0.2
Maximum growth rate of seagrass	μ_{SG}^{max}	d^{-1}	0.1
Maximum growth rate large phytoplankton	μ_{LP}^{max}	d^{-1}	1.25
Maximum growth rate of small phytoplankton	μ_{SP}^{max}	d^{-1}	1.25
Maximum growth rate of microphytobenthos	μ_{MPB}^{max}	d^{-1}	0.35
Maximum growth rate of large zooplankton	μ_{ZL}^{max}	d^{-1}	0.375
Maximum growth rate of small zooplankton	μ_{ZS}^{max}	d^{-1}	3.0
Radius of large phytoplankton	r_{LP}	m	$10 e-6$
Radius of small phytoplankton	r_{SP}	m	$2.5 e-6$
Radius of microphytobenthos	r_{MPB}	m	$10 e-6$
Radius of small zooplankton	r_{ZS}	m	$12.5 e-6$
Radius of large zooplankton	r_{ZL}	m	$50 e-6$
Effective encounter velocity of ZS and PS	$U_{ZS/PS}$	$m s^{-1}$	$1.9 e-4$
Effective encounter velocity of ZL and PL	$U_{ZL/PL}$	$m s^{-1}$	$2.7 e-4$
Effective encounter velocity of ZL and MB	$U_{ZL/MB}$	$m s^{-1}$	$2.7 e-4$
Turbulent kinetic energy dissipation rate	ε	$m^2 s^{-3}$	10^{-6}
Kinematic viscosity	ν	$m^2 s^{-1}$	10^{-6}
Molecular diffusivity of nitrate	D	$m^2 s^{-1}$	17.5×10^{-9}
Effective boundary layer thickness	δ	mm	0.063

Notes: k_w , k_{DON} and k_{DL} from Murray and Parslow (1997); k_{TSS} unpublished data from Gippsland Lakes, Australia; \overline{aA}_{MA} from Enriquez, Agustí, and Duarte (1994); \overline{aA}_{SG} fitted; maximum growth rates within ranges of Murray and Parslow (1997); $\delta = 0.063$ mm from Baird and Atkinson (1997), with friction coefficient, $c_f = 0.005$, water velocity, $U_b = 0.1 m s^{-1}$ and sand-grain roughness length, $k_s = 0.1$ m. Maximum growth rates are within the ranges used in estuarine models (see PPBES), and encounter velocity were based on size dependent rates.

Table 2

For the 70 simulations in Fig. 1; this table gives the parameter to which total water column microalgal biomass is most sensitive. Each column lists the simulations with a specific depth of the lagoon (m), and each row lists the simulations with a specific point source nutrient load specified per unit area ($mg N m^{-2} d^{-1}$). The number in brackets is the normalized relative sensitivity of the listed parameter. Definition of parameters is given in Table 3

Load	Depth				
	2	3	5	10	20
0.1	$r_{ZS}(1.43)$	$r_{ZS}(1.05)$	$r_{ZS}(0.55)$	$r_{ZL}(0.46)$	$r_{ZL}(0.72)$
1	$r_{ZS}(1.35)$	$r_{ZS}(0.85)$	$r_{ZS}(0.42)$	$r_{ZL}(0.49)$	$r_{ZL}(0.75)$
2	$r_{ZS}(1.13)$	$r_{ZS}(0.63)$	$r_{ZS}(0.34)$	$r_{ZL}(0.53)$	$r_{ZL}(0.78)$
3	$r_{ZS}(0.60)$	$r_{ZS}(0.48)$	$r_{ZL}(0.39)$	$r_{ZL}(0.55)$	$r_{ZL}(0.81)$
4	$r_{ZS}(0.63)$	$r_{ZS}(0.43)$	$r_{ZL}(0.45)$	$r_{ZL}(0.58)$	$r_{ZL}(0.84)$
5	$r_{ZS}(0.55)$	$r_{ZS}(0.39)$	$r_{ZL}(0.51)$	$r_{ZL}(0.61)$	$r_{ZL}(0.86)$
10	$r_{ZL}(0.79)$	$r_{ZL}(0.75)$	$r_{ZL}(0.75)$	$r_{ZL}(0.77)$	$r_{ZL}(0.97)$
20	$\mu_{ZL}^{max}(-1.60)$	$\mu_{ZL}^{max}(-0.54)$	$r_{ZL}(1.34)$	$r_{ZL}(1.00)$	$r_{ZL}(1.13)$
30	$\mu_{MPB}^{max}(0.71)$	$\mu_{MB}^{max}(-0.58)$	$\mu_{ZL}^{max}(-0.79)$	$r_{ZL}(1.06)$	$r_{ZL}(1.26)$
40	$\mu_{MPB}^{max}(11.25)$	$\mu_{MPB}^{max}(1.31)$	$\mu_{ZL}^{max}(-0.62)$	$\mu_{ZL}^{max}(-2.03)$	$r_{ZL}(1.35)$
50	$k_s(-0.08)$	$\mu_{MPB}^{max}(0.063)$	$\mu_{ZL}^{max}(-0.34)$	$\mu_{ZL}^{max}(-1.79)$	$r_{ZL}(1.37)$
60	$k_s(-0.08)$	$k_s(-0.06)$	$\mu_{ZL}^{max}(-0.06)$	$\mu_{ZL}^{max}(-0.47)$	$\mu_{ZL}^{max}(-1.86)$
80	$\mu_{PL}^{max}(0.10)$	$k_s(-0.06)$	$\mu_{ZL}^{max}(-0.06)$	$\mu_{ZL}^{max}(-0.07)$	$\mu_{ZL}^{max}(-2.36)$
100	$\mu_{PL}^{max}(0.14)$	$k_s(-0.06)$	$\mu_{ZL}^{max}(-0.04)$	$\mu_{ZL}^{max}(-0.10)$	$\mu_{ZL}^{max}(-3.67)$

2.4. Comparison of parameter values between a mechanistic approach and the PPBES ecological model

The Monod growth curve used in the PPBES ecological model is given by:

$$\mu = \frac{\mu^{\max}S}{K_{1/2} + S} \quad (26)$$

where S is the substrate, and could be nitrate, light, etc. and $K_{1/2}$ is a half-saturation constant. The initial slope of Monod growth versus substrate curve, α_e , is given (using the quotient rule) by Healey (1980):

$$\alpha_e = \frac{d}{dS} \Big|_{S=0} \frac{\mu^{\max}S}{K_{1/2} + S} = \frac{\mu^{\max}}{K_{1/2}} \quad (27)$$

In fact, Healey (1980) points out that α_e is a more robust parameter than $K_{1/2}$, although the initial slope has not generally been adopted by ecological modellers. The initial slope of the Monod growth curve, α_e , can be compared to the mechanistically determined rates, α_m , which also represent the initial slope for the growth versus substrate curve. α_m is a calculated physical limit, and cannot be exceeded by a biological process. If $\alpha_e \gg \alpha_m$, the value of the half-saturation constant should be questioned. If $\alpha_m \gg \alpha_e$, the empirical data would suggest that uptake is not operating near its physical limit, and another limit (such as a biochemical one) may be determining the growth rate. If the rates are similar (say within a factor of two or three), the two approaches are probably quantifying the same phenomena by different means.

2.4.1. Maximum nutrient uptake rates by phytoplankton

Table 3 compares the mechanistic calculation of the initial slope of the growth versus nutrient concentration curve based on diffusion to a perfectly absorbing sphere, α_m , with the PPBES ecological model empirical approximation of the initial slope, α_e , for two size classes of phytoplankton. The mechanistic rates of small and large phytoplankton nutrient uptake were 20 and five times greater than the PPBES ecological model (Table 3). This suggests a process not accounted for in the mechanistic formulation (such as enzyme-mediated intracellular processes) is limiting nutrient uptake. However, Port Phillip Bay did not show extreme nutrient stress (the lowest nitrate levels were $\approx 1 \text{ mg N m}^{-3}$), while other Australian estuaries are regularly reduced to below detection limit (such as Wilson Inlet, Western Australia and Gippsland

Lakes, Victoria), suggesting a lower half-saturation constant, perhaps of the order of the diffusion limit. Given this uncertainty, and the desire to have only one processes limiting uptake (instead of a combination of diffusion resistance and enzyme control) the diffusion limit alone was used to calculate α_m . Future work could incorporate a combination of intracellular and diffusional processes (Smith & Walker, 1980).

2.4.2. Maximum light capture rates by phytoplankton

The mechanistic formulation attenuates light due to phytoplankton in the water column at a rate of $n\bar{aA}$, where n is the number of cells. The PPBES model uses a nitrogen-specific attenuation coefficient, which can be compared with the mechanistic absorption cross-section, \bar{aA} , calculation (Eq. (10)) divided by m_N . For small phytoplankton, $m_N = 1.1 \times 10^{-13} \text{ mol N cell}^{-1} = 1.5 \times 10^{-9} \text{ mg N cell}^{-1}$ (Eq. (18)), so $\bar{aA}/m_N = 0.002 \text{ m}^2 \text{ mg N}^{-1}$. For large phytoplankton, $m_N = 2.5 \times 10^{-12} \text{ mol N cell}^{-1} = 3.5 \times 10^{-8} \text{ mg N cell}^{-1}$ (Eq. (18)), so $\bar{aA}/m_N = 0.0013 \text{ m}^2 \text{ mg N}^{-1}$. These are comparable with the PPBES value of $0.0035 \text{ m}^2 \text{ mg N}^{-1}$. Table 4 compares the maximum light uptake based on the absorption cross-section, $\alpha_m = \bar{aA}_{\text{cell}}/m_l$, with the initial slope of phytoplankton growth versus irradiance curve, α_e , used in the PPBES ecological model. The mechanistic calculation of light penetration through the water column and light-limited growth are comparable with the analogous processes in the PPBES ecological model.

2.4.3. Maximum nutrient uptake by macroalgae

The mechanistic calculation of the initial slope of growth rate versus substrate concentration is based on mass transfer limited uptake through an effective boundary layer 0.1 mm thick. The mechanistic calculation of nutrient uptake produces an initial slope of nutrient uptake per square metre, α_m . α_m is based on an areal flux of nutrient uptake, is independent of algal biomass and takes the units of m s^{-1} . In contrast, the empirical approach of the PPBES calculates an initial slope of uptake rate, α_e , which is a linear function of biomass, and has units of $\text{d}^{-1} \text{ mg N}^{-1} \text{ m}^3$. To compare these two approaches, the biomass of macroalgae required by the empirical approach to give the same nutrient uptake as the mechanistic approach is calculated (i.e. $MA = \alpha_m/\alpha_e$). For the mass transfer limited case, $\alpha_m = D/\delta = 19 \times 10^{-10}/10^{-4} = 19 \times 10^{-5} \text{ m s}^{-1}$ (assuming $\delta = 0.1 \text{ mm}$). From the PPBES ecological model, the macroalgae had

Table 3

Comparison of mechanistic and empirical descriptions of maximum nutrient uptake, based on the initial slope of growth versus nutrient concentration

Cell radius (μm)	ψD ($\text{m}^3 \text{ cell}^{-1} \text{ s}^{-1}$)	m_N (Eq. (18)) (mg N cell^{-1})	$\alpha_m = \psi D/m_N$ ($\text{mg N}^{-1} \text{ m}^3$)	$\alpha_e = \mu^{\max}/K_{1/2}$ ($\text{mg N}^{-1} \text{ m}^3$)
2.5	0.60×10^{-13}	0.15×10^{-8}	3.4	0.18
10	2.4×10^{-13}	3.5×10^{-8}	0.59	0.11

Table 4

Comparison of mechanistic and empirical descriptions of maximum light capture, based on the initial slope of growth versus irradiance curve. The absorption coefficient, $\overline{\gamma C}$, of a cell with a chl *a*-specific absorption of $\gamma = 0.05 \text{ m}^2 \text{ mg (chl } a)^{-1}$, and a pigment concentration of $C = 10 \times 10^6 \text{ mg (chl } a) \text{ m}^{-3}$ is $50,000 \text{ m}^{-1}$. $1 \text{ W m}^{-2} = 2.17 \times 10^5 \text{ mol photon m}^{-2} \text{ s}^{-1}$

Cell radius (μm)	γC (m^{-1})	\overline{aA} ($\text{m}^2 \text{ cell}^{-1}$)	m_l (Eq. (18)) (mol cell^{-1})	$\overline{aA}/m_l = \alpha_m$ ($\text{d}^{-1} (\text{W m}^{-2})^{-1}$)	$\alpha_e = \mu^{\text{max}}/K_{1/2}$ ($\text{d}^{-1} (\text{W m}^{-2})^{-1}$)
2.5	50,000	3.0×10^{-12}	7.1×10^{-12}	0.162	0.124
10	50,000	4.7×10^{-1}	4.5×10^{-10}	0.416	0.170

a $K_{1/2}$ of 20 mg N m^{-3} and μ^{max} of 0.1 d^{-1} , so using Eq. (27), $\alpha_e = 5 \times 10^{-3} \text{ d}^{-1} \text{ mg N}^{-1} \text{ m}^3$. The MA biomass that would give equal rates of nutrient uptake per square metre is given by:

$$\text{MA} = \frac{D/\delta}{\mu^{\text{max}}/K_{1/2}} = 3283 \text{ mg N m}^{-2} \quad (28)$$

Above a macroalgae biomass of 3283 mg N m^{-2} , the mechanistic rate calculation would predict a lower nutrient uptake rate than the PPBES, and below 3283 mg N m^{-2} a higher rate. The value of 3283 mg N m^{-2} is a medium density benthic community.

2.4.4. Encounter rates of predators and prey

The biomechanical calculation of the initial slope between grazing rate and prey concentration, ϕ , can be directly compared with the PPBES clearance rate, C , which is an empirical parameter also representing the initial slope of the grazing rate and prey concentration. In the PPBES, clearance rate for small zooplankton (feeding exclusively on small phytoplankton), C_{ZS} , was $0.4 \text{ m}^3 \text{ mg N}^{-1} \text{ d}^{-1}$, where $\text{m}^3 \text{ mg N}^{-1}$ is per phytoplankton biomass. Converting to per cell per second (one $2.5 \mu\text{m}$ cell = $1.5 \times 10^{-9} \text{ mg N}$ using Eq. (18)), $C_{ZS} = 6.9 \times 10^{-15} \text{ m}^3 \text{ cell (P)}^{-1} \text{ s}^{-1}$. As a comparison, the relative motion and shear stress levels required in the mechanistic calculations to obtain the PPBES clearance rates is determined below.

The PPBES clearance rate would be found at a relative velocity (due to sinking and swimming) of small phytoplankton and small zooplankton of (Baird & Emsley, 1999, Table 2):

$$U_{\text{eff}} = \frac{C_{ZS}}{\pi(r_{\text{PS}} + r_{\text{ZS}})^2} = \frac{6.9 \times 10^{-15}}{\pi(2.5 \times 10^{-6} + 12.5 \times 10^{-6})^2} = 10 \mu\text{m s}^{-1} \quad (29)$$

Large phytoplankton cell being grazed by a large zooplankton cell gives:

$$U_{\text{eff}} = \frac{C_{ZL}}{\pi(r_{\text{PL}} + r_{\text{ZL}})^2} = \frac{2.5 \times 10^{-12}}{\pi(10 \times 10^{-6} + 50 \times 10^{-6})^2} = 220 \mu\text{m s}^{-1} \quad (30)$$

Both of these calculated effective swimming velocities are within the range that could be expected of 10 and 50 μm zooplankton preying on 2.5 and 10 μm phytoplankton, respectively, (of up to 10 zooplankton diameters a second).

The PPBES clearance rate for small phytoplankton and small zooplankton would be found at a shear stress, measured as the rate of turbulent kinetic energy dissipation, ε , of Baird & Emsley (1999) (Table 2):

$$\begin{aligned} \varepsilon &= v \left(\frac{C_{ZS}}{1.3(r_{\text{PS}} + r_{\text{ZS}})^3} \right)^2 \\ &= 10^{-6} \left(\frac{6.9 \times 10^{-15}}{1.3(2.5 \times 10^{-6} + 12.5 \times 10^{-6})^3} \right)^2 \\ &= 7.4 \times 10^{-6} \text{ m}^2 \text{ s}^{-3} \end{aligned} \quad (31)$$

Large phytoplankton cell being grazed by a large zooplankton cell gives:

$$\begin{aligned} \varepsilon &= v \left(\frac{C_{ZL}}{1.3(r_{\text{PL}} + r_{\text{ZL}})^3} \right)^2 \\ &= 10^{-6} \left(\frac{2.5 \times 10^{-12}}{1.3(10 \times 10^{-6} + 50 \times 10^{-6})^3} \right)^2 \\ &= 7.9 \times 10^{-5} \text{ m}^2 \text{ s}^{-3} \end{aligned} \quad (32)$$

These are relatively high values for ε , suggesting that only under highly turbulent conditions is shear stress determining grazing rates. Nonetheless, the reasonable values taken by U_{eff} indicate that the clearance rates empirically determined in the PPBES are probably capturing encounter rate-limited phenomena.

In summary, while including mechanistic functional forms aims to replace many of the empirical forms in the PPBES ecological model, the good correspondence between α_m and α_e , and C and ϕ values, respectively, implies that the empirical model was doing a good job of capturing the underlying processes. The mechanistic rates of light capture of phytoplankton, grazing rates and nutrient uptake by macroalgae are consistent with the parameter values used in PPBES. The uptake rates of phytoplankton

seem to be consistently overestimated (by a factor of five and 20) when using the mass transfer limit.

3. Simulations of a coastal lagoon

To illustrate the behaviour of the model over a range of estuarine depths and nutrient loads, 70 simulations were run to a stable annual oscillation (the results of a further 20,880 simulations, and comparison with data sets from five Australian estuaries can be viewed at the CSIRO Simple Estuarine Response Model site: <http://www.marine.csiro.au/serm>). The runs were of one-box coastal lagoons with depths of 2, 3, 5, 10 and 20 m. For each lagoon, 14 nutrient loads of 0.1, 1, 2, 3, 4, 5, 10, 20, 30, 40, 50, 60, 80 and 100 $\text{mg N m}^{-2} \text{d}^{-1}$ were applied. The residence time of the lagoon was 50 days (other SERM parameters were inflow colour = 0.2 m^{-1} , climate zone = uniform rainfall distribution (UNR), freshwater replacement time = 100 days, oceanic flushing time = 100 days, catchment 2% cleared). Simulations were run for 10 years, after which the time-averaged biomass of the state variables in the 10th year was calculated. Fig. 1 plots time-averaged biomass as a function of load (i.e. each point represents a different simulation).

Features which emerge are: (1) the presence of seagrass in shallow water and low loads only; (2) the bloom of benthic macroalgae at intermediate loads being limited by nutrient and light supply; and (3) at high loads the die off of benthic plants due to large-celled algal blooms. This is consistent with a simple conceptual understanding of estuarine eutrophication (Harris et al., 1996).

A sensitivity analysis was undertaken by changing individual parameters by $\pm 10\%$. Following Murray and Parslow (1997), sensitivity is reported as a normalized relative sensitivity (RS) approximately equal to $\partial(\ln S)/\partial D(\ln P)$ where S is the state variable, and P is the parameter. At the specific set of parameter values and forcings at which the sensitivity analysis was undertaken, S is proportional to P^{RS} . A sensitivity analysis was completed for a subset of model parameters which are emphasized in this paper ($\mu_{\text{SP}}^{\text{max}}$, $\mu_{\text{LP}}^{\text{max}}$, $\mu_{\text{MPB}}^{\text{max}}$, $\mu_{\text{MA}}^{\text{max}}$, $\mu_{\text{SG}}^{\text{max}}$, $\mu_{\text{ZS}}^{\text{max}}$, $\mu_{\text{ZL}}^{\text{max}}$, r_{SP} , r_{LP} , r_{MPB} , r_{ZS} , r_{ZL} , γ_{CSP} , γ_{CLP} , γ_{CMPB} , aA_{MA} , aA_{SG} , ε , $U_{\text{ZS/PS}}$, $U_{\text{ZL/PL}}$, $U_{\text{ZL/MPB}}$, c_{f} , U_{b} and k_{s}). As the sensitivity of parameters changes depending on the forcing, the sensitivity analysis was completed for each of the 70 simulations. Table 2 lists the parameter to which water column microalgal biomass is most sensitive, and its normalized relative sensitivity, for all 70 different simulations in Fig. 1. The sensitivity

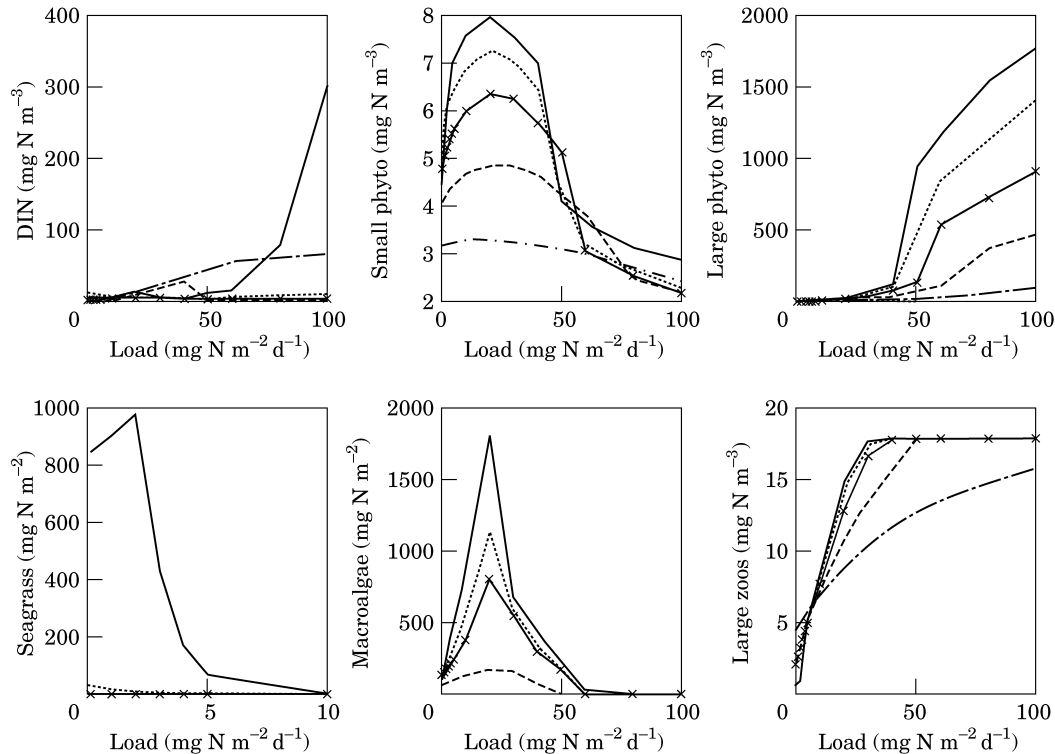


Fig. 1. The biomass of autotrophs in five simulated coastal lagoons (with depths of 2, 3, 5, 10 and 20 m) versus increasing nutrient loads. The lines join simulations at nutrient loads of 0.1, 1, 2, 3, 4, 5, 10, 20, 30, 40, 50, 60, 80 and 100 $\text{mg N m}^{-2} \text{d}^{-1}$ for each depth. Each graph depicts, in the clockwise direction from the top left, the annual average of the following model state variables: water column dissolved inorganic nitrogen concentration (mg N m^{-3}), small phytoplankton ($r = 2.5 \mu\text{m}$) biomass (mg N m^{-3}), large phytoplankton ($r = 10 \mu\text{m}$) biomass (mg N m^{-3}), seagrass biomass (mg N m^{-2}), benthic macroalgae biomass (mg N m^{-2}), large zooplankton ($r = 50 \mu\text{m}$) biomass (mg N m^{-3}).

of water column microalgal biomass varies from being most sensitive to the physical size of grazers at low loads, to depending primarily on growth rates of phytoplankton and zooplankton at high loads.

4. Discussion

4.1. The mechanistic approach

When compared to commonly used empirical descriptions, the mechanistic approach results in significantly different functional forms for describing autotrophic growth. The most significant difference between the mechanistic and empirical approaches was in the representation of macroalgal growth. In the PPBES ecological model (as well as Madden & Kemp, 1996 and other models), growth rate of macroalgae is an exponential function of the biomass of the autotroph under all nutrient and light levels. In contrast, the mechanistic formulation requires that the rate of biomass increase varies from being an exponential function of biomass at nutrient and light-saturating conditions ($\Delta MA = \mu_{MA}^{\max}$), to being independent of biomass at nutrient-limiting conditions ($\Delta MA \propto DN/\delta$), to having a complex exponential relationship with biomass at light-limiting conditions ($\Delta MA \propto I_{\text{bot}}(1 - e^{-a_{MA}MA})$).

The mechanistic approach uses a set of parameter values quite different from the empirical approach. Significantly, half-saturation constants, which are often both poorly constrained, and can impact significantly on model output (Murray & Parslow, 1997) are replaced by parameters with very specific physical interpretations. These parameters can often be measured accurately, and in many cases, will take similar values in all estuaries. The biggest disadvantage of the mechanistic approach is the underlying assumption that all important processes have been captured. Empirical models, while perhaps theoretically less attractive, are constrained by observations. The empirical descriptions of ecological processes need not represent an accurate or complete description of the system being modelled. As long as the empirical model behaviour does not deviate far from the calibration data set, the model should perform well. The mechanistic approach, in contrast, does rely on the modeller capturing the important processes. Another disadvantage of the mechanistic approach is the introduction of a new parameter set. While mechanistic parameters can be constrained by theoretical interpretations, this exercise has received little attention in the literature. In contrast, empirical models have been well explored, and literally hundreds of estimations of parameter values undertaken (i.e. Hamilton & Schladow, 1997).

The choice between mechanistic and empirical descriptions in an ecological model should depend on the

purpose of the model, the understanding of processes within the system and the data available. This model was developed for a broad look at autotrophic responses in the Australian continents approximately 1000 estuaries: the variety of environments and lack of data justifying a mechanistic approach. Nonetheless, it is expected that some of the mechanistic equations developed here will be useful for complex ecological models of estuaries with comprehensive data sets.

4.2. Comparison with simple conceptual model of estuarine eutrophication

A common conceptual understanding of estuarine eutrophication is the switch from biomass being dominated by slow-growing plants to fast-growing planktonic algal cells with increasing nutrient loads (Harris, 1999; Harris et al., 1996). The model of estuarine eutrophication presented in this paper captures the switch from slow-growing benthic plants to fast-growing algal cells, revealing some of the underlying physical processes that control the ecological response of estuarine systems. In particular, the presented model is based on maximum uptake calculations which depend on the morphology and location of the autotroph, while quantifying the autotroph's intracellular processes with a single growth rate parameter for each autotroph. The model nonetheless followed the simple conceptual model of eutrophication mentioned above. This suggests that the ecological responses of estuarine systems to nutrient loads (which are fairly ubiquitous), are determined, to a significant degree, by the physical properties of the autotrophs and their maximum growth rates.

5. Conclusions

This paper presented a new model of estuarine eutrophication. Key processes involved in estuarine eutrophication such as nutrient uptake and light capture of autotrophs and predator–prey interactions were represented by more mechanistic descriptions than commonly employed. A comparison of mechanistic and empirical process rate calculations demonstrated similarities in outputs between the two approaches and sheds light on the meaning of the parameters values chosen in empirical models. This framework provided a prognostic model of eutrophication which is compatible with a simple conceptual understanding of eutrophication, and that worked over a broad range of estuarine environmental forcings. Further developed, the use of mechanistic descriptions in models of estuarine eutrophication may provide predictive capabilities beyond the present suite of models with empirical descriptions and more thoroughly test our knowledge of the workings of estuarine systems.

Acknowledgements

This work contributed to Theme 7 (Ecosystem Health)—Estuaries, Task 4 of the National Land and Water Resources Audit, a programme of the Natural Heritage Trust (NHT), Australia, and has been undertaken by CSIRO in partnership with the CRC for Coastal Zone, Estuary and Waterway Management. The support of NHT is gratefully appreciated. Thanks to Francesco di Pierro and Jason Waring for their modelling support, and Phillip Ford, Myriam Bormans and four anonymous reviewers for their insights.

References

- Baird, M. E., & Atkinson, M. J. (1997). Measurement and prediction of mass transfer to experimental coral reef communities. *Limnology and Oceanography* 42, 1685–1693.
- Baird, M. E., & Emsley, S. M. (1999). Towards a mechanistic model of plankton population dynamics. *Journal of Plankton Research* 21, 85–126.
- Baird, M. E., Emsley, S. M., & McGlade, J. M. (2001). Modelling the interacting effects of nutrient uptake, light capture and temperature on phytoplankton growth. *Journal of Plankton Research* 23, 829–840.
- Boudreau, B. P. (1996). The diffusive tortuosity of fine grained un-lithified sediments. *Geochimica et Cosmochimica Acta* 60, 3139–3142.
- Bricker, S. B., Clement, C. G., Pirhalla, D. E., Orlando, S. P., & Farrow, D. R. G. (1999). *National estuarine eutrophication assessment: effects of nutrient enrichment in the nation's estuaries*. Silver Spring, MD: Technical report NOAA, National Ocean Service. Special Projects Office for Coastal Ocean Science.
- Chorus, I., & Bartram, J. (Eds.) (1999). *Toxic cyanobacteria in water*. London: E and FN Spon.
- Cloern, J. E. (2001). Our evolving conceptual model of the coastal eutrophication problem. *Marine Ecology Progress Series* 210, 223–253.
- Droop, M. R. (1968). Vitamin B-12 and marine ecology IV. The kinetics of uptake, growth and inhibition in *Monochrysis lutheri*. *Journal of the Marine Biological Association of the United Kingdom* 48, 689–733.
- Enriquez, S., Agustí, S., & Duarte, C. M. (1994). Light absorption by marine macrophytes. *Oecologia* 98, 121–129.
- Fasham, M. J. R., Ducklow, H. W., & McKelvie, S. M. (1990). A nitrogen-based model of plankton dynamics in the oceanic mixed layer. *Journal of Marine Research* 48, 591–639.
- Fong, P., Kamer, K., Boyer, K. E., & Boyle, K. A. (2001). Nutrient content of macroalgae with differing morphologies may indicate sources of nutrients for tropical marine systems. *Marine Ecology Progress Series* 220, 137–152.
- Hamilton, D. P., & Schladow, S. (1997). Prediction of water quality in lakes and reservoirs. Part I—model description. *Ecological Modelling* 96, 91–110.
- Harris, G. (1999). Comparison of the biogeochemistry of lakes and estuaries: ecosystem processes, functional groups, hysteresis effects and interactions between macro- and microbiology. *Marine and Freshwater Research* 50, 791–811.
- Harris, G., & Batley, G., et al. (1996). *Port Phillip Bay Environmental Study Final Report*. CSIRO, Canberra, Australia.
- Healey, F. P. (1980). Slope of the Monod equation as an indicator of advantage in nutrient competition. *Microbial Ecology* 5, 281–286.
- Hofmann, M., Wolf-Gladrow, D. A., Takahashi, T., Sutherland, S. C., Six, K. D., & Maier-Reimer, E. (2000). Stable carbon isotope distribution of particulate organic matter in the ocean: a model study. *Marine Chemistry* 72, 131–150.
- Hurd, C. L. (2000). Water motion, marine macroalgal physiology, and production. *Journal of Phycology* 36, 453–472.
- Jackson, G. A. (1995). Coagulation of marine algae. In C. P. Huang, C. R. O'Melia, & J. J. Morgan (Eds.), *Aquatic chemistry: Interfacial and interspecies processes* (pp. 203–217). Washington, DC: American Chemical Society.
- Kirk, J. T. O. (1975). A theoretical analysis of the contribution of algal cells to the attenuation of light within natural waters. II. Spherical cells. *New Phytologist* 75, 21–36.
- Madden, C. J., & Kemp, W. M. (1996). Ecosystem model of an estuarine submersed plant community: calibration and simulation of eutrophication responses. *Estuaries* 19, 457–474.
- Murray, A., & Parslow, J. (1997). *Port Phillip Bay integrated model: final report*. Canberra, A.C.T.: Technical report CSIRO.
- Nixon, S. W. (1995). Coastal marine eutrophication—a definition, social causes and future concerns. *Ophelia* 41, 199–219.
- Pasciak, W. J., & Gavis, J. (1975). Transport limited nutrient uptake rates in *Dictylum brightwellii*. *Limnology and Oceanography* 20, 604–617.
- Riber, H. H., & Wetzel, R. G. (1987). Boundary-layer and internal diffusion effects on phosphorus fluxes in lake periphyton. *Limnology and Oceanography* 32, 1181–1194.
- Sanford, L. P., & Crawford, S. M. (2000). Mass transfer versus kinetic control of uptake across solid–water boundaries. *Limnology and Oceanography* 45, 1180–1186.
- Smith, F. A., & Walker, N. A. (1980). Photosynthesis by aquatic plants: effects of unstirred layers in relation to assimilation of CO₂ and HCO₃ and to carbon isotopic discrimination. *New Phytologist* 86, 245–259.
- Steele, J. H., & Clark, C. W. (1998). Relationship between individual- and population-based plankton models. *Journal of Plankton Research* 20, 1403–1415.
- Strathmann, R. R. (1967). Estimating the organic carbon content of phytoplankton from cell volume or plasma volume. *Limnology and Oceanography* 12, 411–418.